

# Non-Stationary Stochastic Optimization of an Oscillating Water Column

María L. Jalón, Feargal Brennan

**Abstract**—A non-stationary stochastic optimization methodology is applied to an OWC (oscillating water column) to find the design that maximizes the wave energy extraction. Different temporal cycles are considered to represent the long-term variability of the wave climate at the site in the optimization problem. The results of the non-stationary stochastic optimization problem are compared against those obtained by a stationary stochastic optimization problem. The comparative analysis reveals that the proposed non-stationary optimization provides designs with a better fit to reality. However, the stationarity assumption can be adequate when looking at averaged system response.

**Keywords**—Non-stationary stochastic optimization, oscillating water column, temporal variability, wave energy.

## I. INTRODUCTION

SINCE the last decades, wave energy is being investigated as an alternative to fossil fuels [1]–[3]. Of the wave energy converters, the OWC (oscillating water column) system is the most studied and the one with the largest number of full-size prototypes [4]. However, these systems are not yet competitive and several researchers have tried to find the optimal designs among all possible. López et al. [5] used a numerical model to maximize the capture factor of a fixed OWC for a given set of wave conditions. Gomes et al. [6] maximized the annual average power available to the turbine of a floating OWC device from real sea waves, using a stochastic model [7]. Jalón et al. [8] described a stochastic optimization framework for an OWC in different time scales (season, year). Furthermore, they considered time-series simulations of the wave climate taking into account its temporal variability [9], [10] to compare the future performance of the different optimal designs obtained with the stochastic optimization.

Notwithstanding, the temporal variability of the wave climate should also be considered in the design of such devices, because of the influence of the variability of wave energy on the power output [11]. In this context, the main research objective of this paper is to describe and analyse the non-stationary stochastic optimization for an OWC. For this purpose, non-stationary mixture distributions of the peak period are used in the optimization method proposed by Jalón et al. [8].

## II. METHODOLOGY

For this research, we consider a particular design for an OWC system (Fig. 1) with radius  $a$ , submergence  $d$ , and

María L. Jalón. Offshore Renewable Energy Engineering Centre, Cranfield University, Cranfield, Bedfordshire MK43 0AL, UK (corresponding author, e-mail: m.l.jalon@cranfield.ac.uk).

Feargal Brennan. Offshore Renewable Energy Engineering Centre, Cranfield University, Cranfield, Bedfordshire MK43 0AL, UK.

emergence  $e$ . This device has a Wells turbine with an outer rotor diameter  $D$ , and rotational speed  $N$ . The system is supposed to be able to automatically modify its parameters ( $d$ ,  $N$ ) so as to maximize the wave energy extraction. To this end, the formula of the available pneumatic power for the turbine in the sea state is adopted to quantify the wave energy extraction.

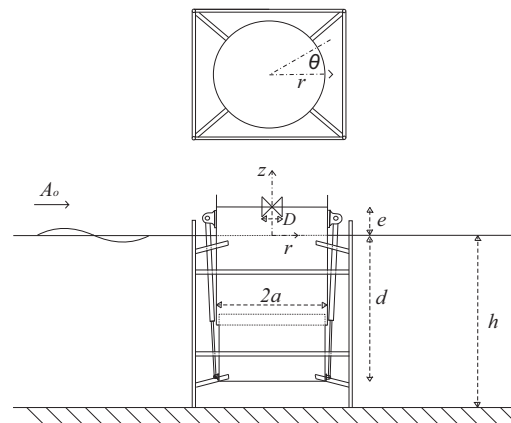


Fig. 1 Sketch of the OWC system [8]

Assuming that values of the submergence and rotational speed of the turbine for which device performance is optimal are weakly depend on significant wave height [8], the stochastic optimization of the wave energy extraction can be calculated as follow:

$$\begin{aligned} \max E[\bar{P}_{avai,irr}] &= \int_{\mathbb{R}} \bar{P}_{avai,irr} f(T_p) dT_p \\ \text{s.t} & \\ 2.0 \leq d &\leq 8.0 \\ 0.0 < N &\leq 2.0 M_{max} c_a / D \end{aligned} \quad (1)$$

where  $\bar{P}_{avai,irr}$  is the available pneumatic power for the turbine in the sea state (see [8]),  $f(T_p)$  is the stationary probability density function of the peak period,  $M_{max}$  is the Mach number, and  $c_a$  is the speed of sound in the air.

However, the temporal variability of the wave climate ( $f(T_p, t)$ ) should be considered in the design of such devices. Hence, under non-stationary conditions, the

optimization problem in (1) rewrites as:

$$\begin{aligned} \max E[\bar{P}_{avai,irr}] &= \int_{\mathfrak{R}} \bar{P}_{avai,irr} f(T_p, t) dT_p, \forall t \in \mathcal{T} \\ \text{s.t} & \\ 2.0 \leq d \leq 8.0 & \\ 0.0 < N \leq 2.0 M_{max} c_a / D & \end{aligned} \quad (2)$$

with  $\mathcal{T}$  being the time window of the data.

For this purpose, a non-stationary parametric mixture model that combines two Log-Normal probability density functions of the peak period [10] is used:

$$f(T_p, t) = \alpha(t) f_{LN_1}(T_p, t) + (1 - \alpha(t)) f_{LN_2}(T_p, t) \quad (3)$$

where  $f_{LN_i}(T_p, t), i = 1, 2$  are the Log-Normal probability density functions, and  $\alpha(t)$  and  $(1 - \alpha(t))$  provides the weight of the first and second Log-Normal distribution with time, respectively. This parametric model is able to reproduce the statistical variability at different time scales. The intra-annual and inter-annual variations of all the parameters of the model ( $\alpha(t), \mu_1(t), \sigma_1(t), \mu_2(t), \sigma_2(t)$ ), are expressed as the superposition of a Fourier truncated series over a time interval of one year, and two longer-term sinusoidal cycles representative of the studied site ( $T_1, T_2$ ):

$$\begin{aligned} \theta(t) &= \theta_0 + \sum_{k=1}^{N_k} [\theta_a^k \cos(2\pi kt) + \theta_b^k \sin(2\pi kt)] \\ &+ \theta_{a1} \cos(2\pi t/T_1) + \theta_{b1} \sin(2\pi t/T_1) \\ &+ \theta_{a2} \cos(2\pi t/T_2) + \theta_{b2} \sin(2\pi t/T_2) \end{aligned} \quad (4)$$

### III. RESULTS

#### A. Intra-Annual and Inter-Annual Variability of the Peak Period

The proposed non-stationary stochastic optimization problem is exemplified for a particular geographical location. The study area is located at a depth of 10.0 m in the Gulf of Cadiz (Spain) (see [8]). Figs. 2 and 3 represent the intra-annual and the inter-annual time variation of the peak period in the site, respectively. From these figures, it can be observed an intra-annual and an inter-annual variation in both the median (red line) and the dispersion (blue box). These analyses show the need to consider the temporal variability in the design of the system.

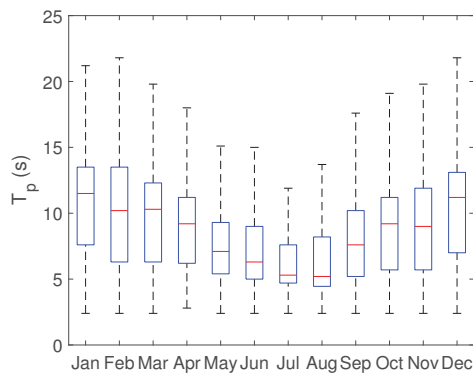


Fig. 2 Intra-annual variability of the peak period

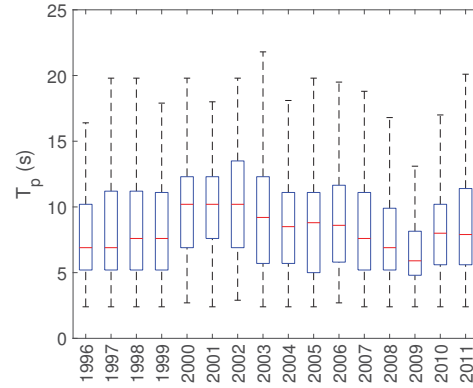


Fig. 3 Inter-annual variability of the peak period

#### B. Parametric Mixture Models

1) *Parametric Stationary Mixture Model*: In the case of the parametric stationary mixture model of the peak period (5), the parameters of the model are not time dependent.

$$f(T_p) = \alpha f_{LN_1}(T_p) + (1 - \alpha) f_{LN_2}(T_p) \quad (5)$$

They are obtained using maximum likelihood ( $\alpha = 0.4345$ ,  $\mu_1 = 1.6507$ ,  $\sigma_1 = 0.2152$ ,  $\mu_2 = 2.3785$ ,  $\sigma_2 = 0.2360$ ), although it could be also calculated from the non-stationary probability density function ( $f(T_p) = \int_0^t f(T_p, t) dt$ ).

To compare the use of a mixture model, the peak period is fitted using a Log-Normal probability density function ( $\mu = 2.062, \sigma = 0.426$ ). Fig. 4 shows both stationary models, along with the empirical probability density function of the peak period. The mixture model (2 Log-Normal) is shown to provide a better fit than the standard model (1 Log-Normal).

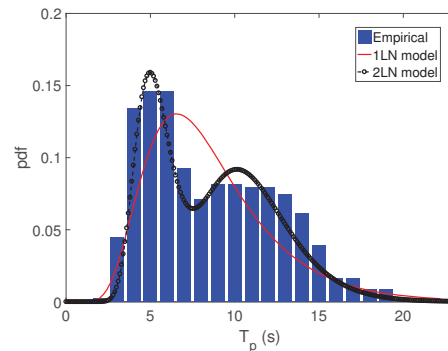


Fig. 4 Empirical probability density function (bins), and probability density function calculated with the standard model (—) and with the mixture model (o), for the peak period

2) *Parametric Non-Stationary Mixture Model*: Fig. 5 shows the non-stationary probability density function fitted to the peak period (3). The inter-annual variations are modeled with cyclical components of  $T_1 = 5$  and  $T_2 = 11$  yrs. The fitting parameters (4) can be found in Jalón et al. [8].

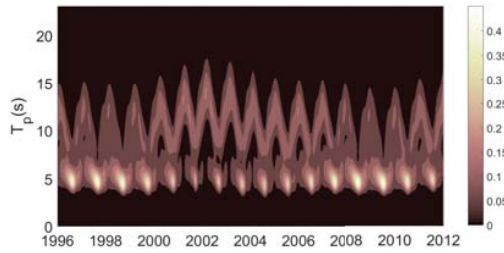


Fig. 5 Non-stationary probability density function of the peak period

Fig. 6 shows both the non-stationary and the stationary probability density function (*pdf*) of the peak period. In the case of the non-stationary function, a different *pdf* is obtained in each period of time. In contrast, the stationary function is represented by the same *pdf* independently of the time.

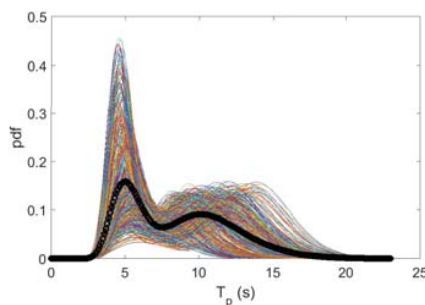


Fig. 6 Non-stationary (—) and stationary (o) probability density function of the peak period

3) *Models Comparison*: In order to understand the influence of taking account the climate variability in the parametric mixture model, the monthly moving average of the data ( $T_p$ ), and the mean values obtained with the different mixture models (non-stationary, stationary) are compared (Fig. 7). The mixture stationary model (2 Log-Normal) provides a constant value for the mean of  $T_p$  along the time. The incorporation of the intra-annual variations in the non-stationary model produces a seasonal change on the mean of  $T_p$ , although its amplitude remains constant along the time. Whereas, the inclusion of the inter-annual variations in the non-stationary model generates a change of the value for the mean of  $T_p$  in cycles longer than one year.

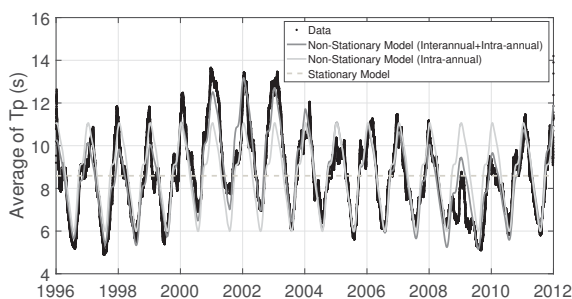


Fig. 7 Monthly average moving of the peak period observed, and the mean of the peak period simulated by the non-stationary and the stationary parametric mixture models

### C. Optimization

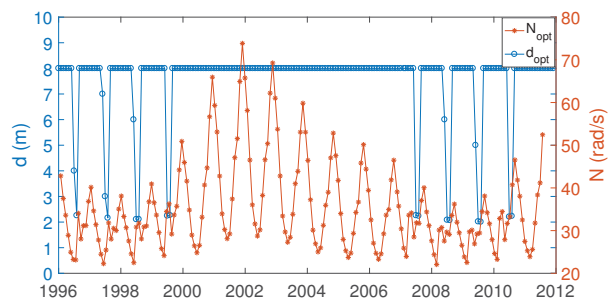
For the optimization process, we consider a value of the turbine diameter  $D = 1$  m, radius  $a = 3.5$  m, and emergence  $e = 5$  m. In regard to the spectrum of the sea states necessary to calculate the available pneumatic power for the turbine in the sea state [8], a constant value of the significant wave height is assumed ( $H_s = 1$  m).

1) *Stationary Stochastic Optimization*: Solving the optimization problem (1) with the mixture and standard stationary probability density functions of the peak period (Fig. 4), the estimated values of the optimal submergence,  $d_{opt}$ , and the optimal rotational speed of the turbine,  $N_{opt}$ , are given in Table I:

model	$d_{opt}(m)$	$N_{opt}(rad/s)$
1 Log-Normal	8	28
2 Log-Normal	8	33

Note that, the same value of the  $d_{opt}$ , which coincides with the maximum submergence imposed, is obtained with the different stationary models (1 Log-Normal, 2 Log-Normal). In regard to  $N_{opt}$ , very similar values are obtained with both models, although the maximum allowed value is not reached.

2) *Non-Stationary Stochastic Optimization*: Following the optimization problem (2) with the non-stationary mixture probability density function of the peak period (Fig. 5), the optimal submergence values,  $d_{opt}$ , and the optimal rotational speed values,  $N_{opt}$ , are obtained based on the time (Fig. 8).

Fig. 8 Results of the non-stationary stochastic optimization:  $d_{opt}$  (o),  $N_{opt}$  (\*)

As can be observed, the optimal results inherit the temporal variability of the wave climate. An intra-annual cycle is observed on the  $N_{opt}$ , where the less energetic months (see Fig. 2) correspond to lower values of  $N_{opt}$ . Furthermore,  $N_{opt}$  presents an inter-annual cycle, reaching the higher values in the higher energetic years (see Fig. 3). In regard to  $d_{opt}$ , an intra-annual cycle is only observed in the less energetic years.

### D. Models Comparison

The available pneumatic power based on the different optimization results and on the wave climate is calculated to compare the performance of the non-stationary and stationary optimal designs (Fig. 9). The values for the

available pneumatic power in each sea state associated with the central regimen, result to be very similar independently of the type of optimization adopted for optimal design (stationary or non-stationary). However, the resulting design from non-stationary optimization provides higher values for pneumatic power.

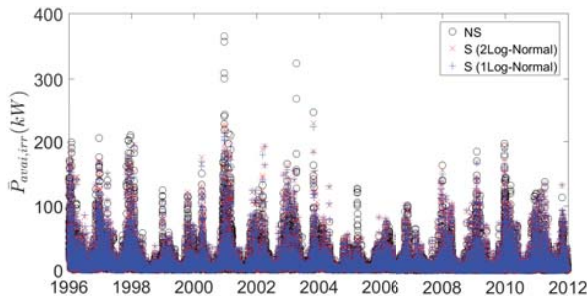


Fig. 9 State curve of the available pneumatic power for an OWC with different designs: non-stationary optimal design (o), stationary optimal design following the 2 Log-Normal model (x), and stationary optimal design following the 1 Log-Normal model (+)

Fig. 10 represents the annual maximum values of the available pneumatic power for the different optimal designs. The higher difference appears in December 2000, where the consideration of the stationary optimal design supposes a decrease of the 37.8 % (2 Log-Normal model) and the 41.3 % (1 Log-Normal model) respect to the non-stationary optimal design.

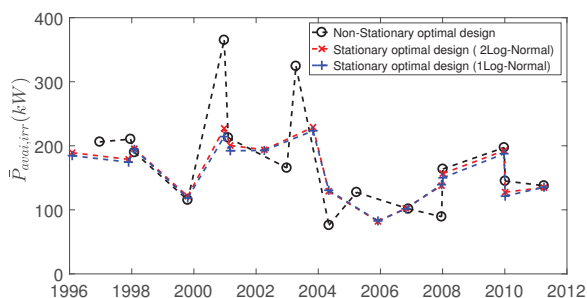


Fig. 10 Annual maximum values of the available pneumatic power for an OWC with different designs: non-stationary optimal design (o), stationary optimal design following the 2 Log-Normal model (x), and stationary optimal design following the 1 Log-Normal model (+)

#### IV. CONCLUSION

This paper proposes a non-stationary stochastic optimization methodology which takes into account the temporal variability of the wave climate in the design of systems whose performance depends on the sequence of the sea states.

The non-stationary stochastic optimization methodology has been applied to an OWC system located in a specific site. As evident from the results, the optimal design variables obtained from the proposed methodology capture the temporal variability of the wave climate, in contrast to the resulting fixed values for these variables given by the stationary optimization. From a practical point of view, this methodology allows a better fit to reality which is intended to avoid a system performance far from optimal along the time. This

better performance is observed in the higher values for wave energy extraction given by the non-stationary optimal design. Notwithstanding, it is noted that the stationarity can be an adequate assumption when looking at averaged system response.

#### ACKNOWLEDGMENT

The authors would like to acknowledge the support of the UK Centre for Marine Energy Research (UKCIMER) under the SuperGen Marine programme funded by the Engineering and Physical Sciences Research Council (EPSRC), Grant EP/P008682/1.

#### REFERENCES

- [1] Fadaeenejad M., Shamsipour R., Rokni S. D., Gomes C. New approaches in harnessing wave energy: With special attention to small islands, *Renewable and Sustainable Energy Reviews* 29 (2014) 345–354.
- [2] Astariz S., Iglesias G. The economics of wave energy: A review, *Renewable and Sustainable Energy Reviews* 45 (2015) 397–408.
- [3] Cuadra L., Salcedo-Sanz S., Nieto-Borge J.C. Alexandre E., Rodríguez G. Computational intelligence in wave energy: Comprehensive review and case study, *Renewable and Sustainable Energy Reviews* 58 (2016) 1223–1246.
- [4] Falcão A. F. O., Henriques J. C. C. Oscillating-water-column wave energy converters and air turbines: A review, *Renewable Energy* 85 (2016) 1391–1424.
- [5] López I., Pereiras B., Castro F., Iglesias G. Optimisation of turbine-induced damping for an OWC wave energy converter using a RANS–VOF numerical model, *Applied Energy* 127 (2014) 105–14.
- [6] Gomes R. P. F., Henriques J. C. C., Gato L. M. C., Falcão A. F. O. Hydrodynamic optimization of an axisymmetric floating oscillating water column for wave energy conversion, *Renewable Energy* 44 (2012) 328–39.
- [7] Falcão A. F. O., Rodrigues R. J. A. Stochastic modelling of OWC wave power plant performance, *Applied Ocean Research* 24 (2) (2002) 59–71.
- [8] Jalón M. L., Baquerizo A., Losada M. A. Optimization at different time scales for the design and management of an oscillating water column system, *Energy* 95 (2016) 110–123.
- [9] Solari S., Losada M. A. Non-stationary wave height climate modeling and simulation, *Journal of Geophysical Research: Oceans* (1978–2012) 116 (C9).
- [10] Solari S., van Gelder P. H. A. J. M. On the use of Vector Autoregressive (VAR) and Regime Switching VAR models for the simulation of sea and wind state parameters, *Marine Technology and Engineering. CENTEC Anniversary Book*, 2011.
- [11] Carballo R., Iglesias G. A methodology to determine the power performance of wave energy converters at a particular coastal location, *Energy Conversion and Management* 61 (2012) 8–18.